Abnormal Podocyte Mechanosensing and Responsiveness Leads to Reduced Structural Integrity of Glomeruli in Two Mouse Models of Podocyte Injury

Supplemental Material

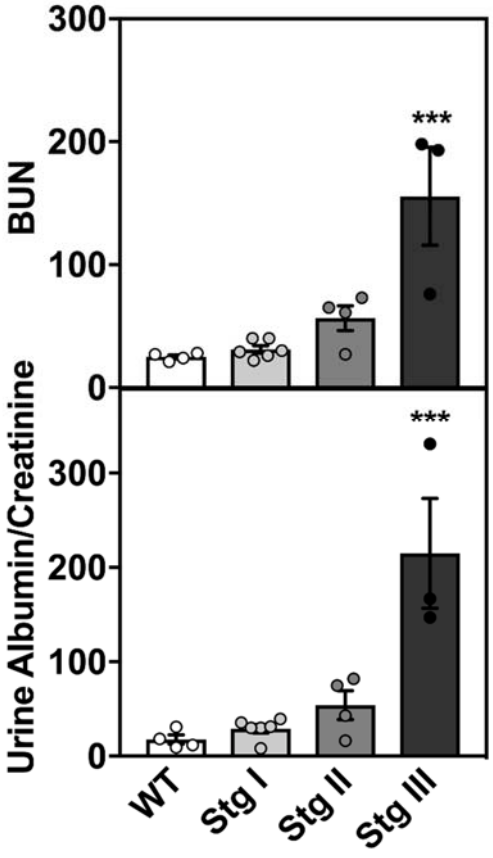

Figure S1. Renal function of Tg26 mice at stages I-III compared to WT age-matched control mice. Renal function as measured by blood urea nitrogen (BUN) and proteinuria measured as albumin/creatinine ratio levels. Disease stages are indicated; $n \geq 6$ for each bar, ***$P<0.001$ compared to WT by ANOVA followed by Dunnett's multiple comparisons test.

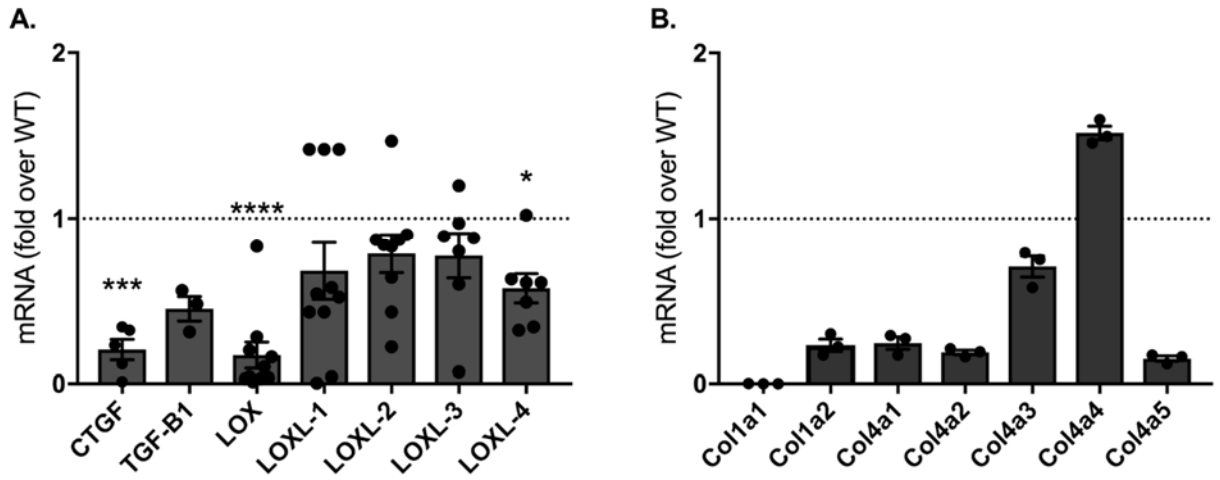

Figure S2. Quantitative RT-PCR measurement of selected mRNAs relevant to fibrosis and scarring from Tg26 podocytes compared to WT control (1.0). Levels are fold differences compared to WT and expressed as fold change from internal GAPDH control, mean ± SE. A) CTGF and LOX and LOXL-4 are significantly less than control (*P<0.05, ***P<0.001, ****P<0.0001 by ANOVA). B) All values are significantly different from control (P<0.0001). These results indicate that the source of collagen in Stage II and Stage III glomeruli is unlikely to be Tg26 podocytes. With disease progression and the complex inflammatory state of the disease, the collagen could come from mesangial cells, other renal cells, or infiltrating cells.

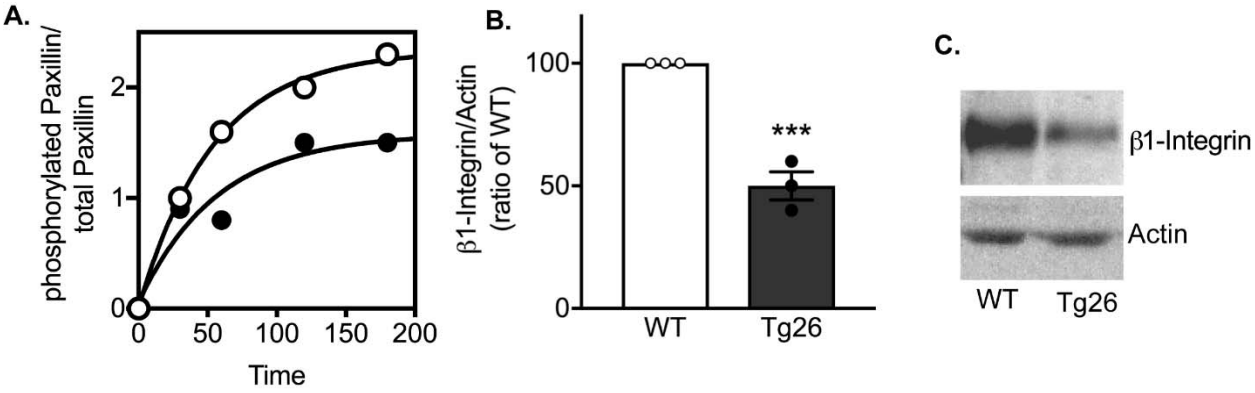

Figure S3. Properties of primary podocytes isolated from Stage II mice. A) Time course of paxillin phosphorylation following plating in WT (white circles) compared to Tg26 (black circles) from WT or primary podocytes Stg II disease kidneys). B) Quantification of β1-integrin protein expression in Tg26 primary podocytes compared to WT. Average of 3 samples are shown ± SE. ***P<0.001 by t-test. Representative immunoblot for β1-integrin and actin in WT and Tg26 primary podocytes (WT or Stg II Tg26 kidneys).

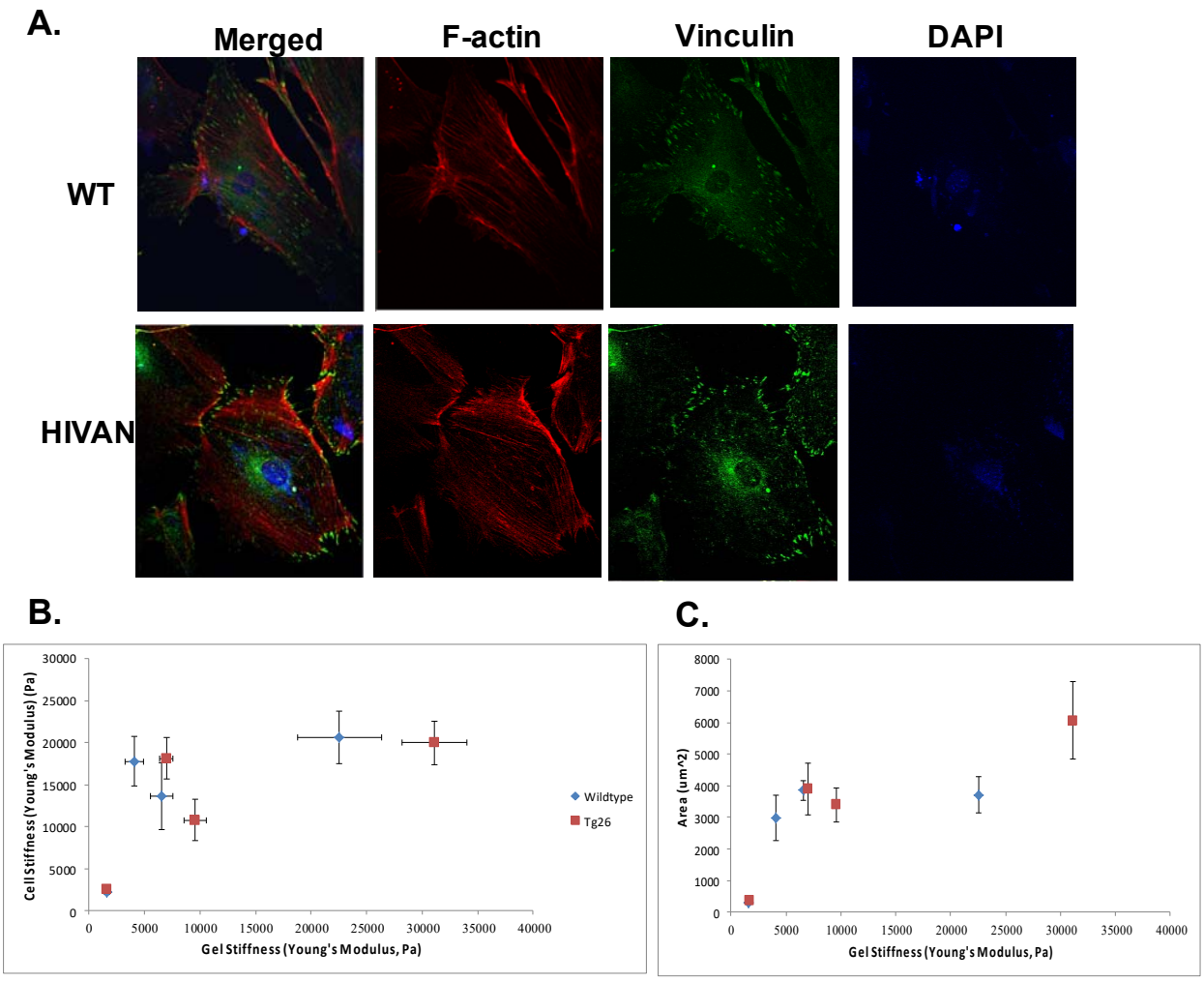

Figure S4. Confirmation that Tg26 glomerular deformability is not due to effects on mesangial cells. The integrated HIV-1 viral genome was present in Tg26 mesangial cells, but not *Nef* mRNA. A) Structure of WT and Tg26 mesangial cells stained with rhodamine-phalloidin (red, F-actin), vinculin (green, focal adhesions), and blue (DAPI, nuclei) and imaged with confocal microscopy at 40X. Lack of structural differences confirm reports that mesangial cells are not infected with HIV-1 in human HIVAN and the Tg26 mouse model does not express the HIV transgene in mesangial cells. B) The stiffening response of normal (blue squares) and Tg26 (red squares) mesangial cells as a function of matrix stiffness. Cells were grown on type I collagen coated acrylamide gels ranging in Young's modulus value from 0.3 to 35 kPa. The Young's modulus of each cell was measured using AFM (6 – 8 measurements) and the region of matrix around the cell was also measured (6 – 8 measurements). Error bars represent mean ± SD. C) Cell spreading response of WT (green diamonds) and Tg26 (blue squares) mesangial cells as a function of matrix stiffness. Cells were grown on type I collagen coated acrylamide gels as above. The area of each cell was measured using Image J (4–5 measurements per cell), and the Young's modulus of the region of matrix around the cell was measured with AFM (6 – 8 measurements). Horizontal error bars represent mean values of matrix Young's modulus

± SD, and vertical error bars represent larger populations of cells (n = 30-50) within gels of the average stiffness shown on the Y axis.

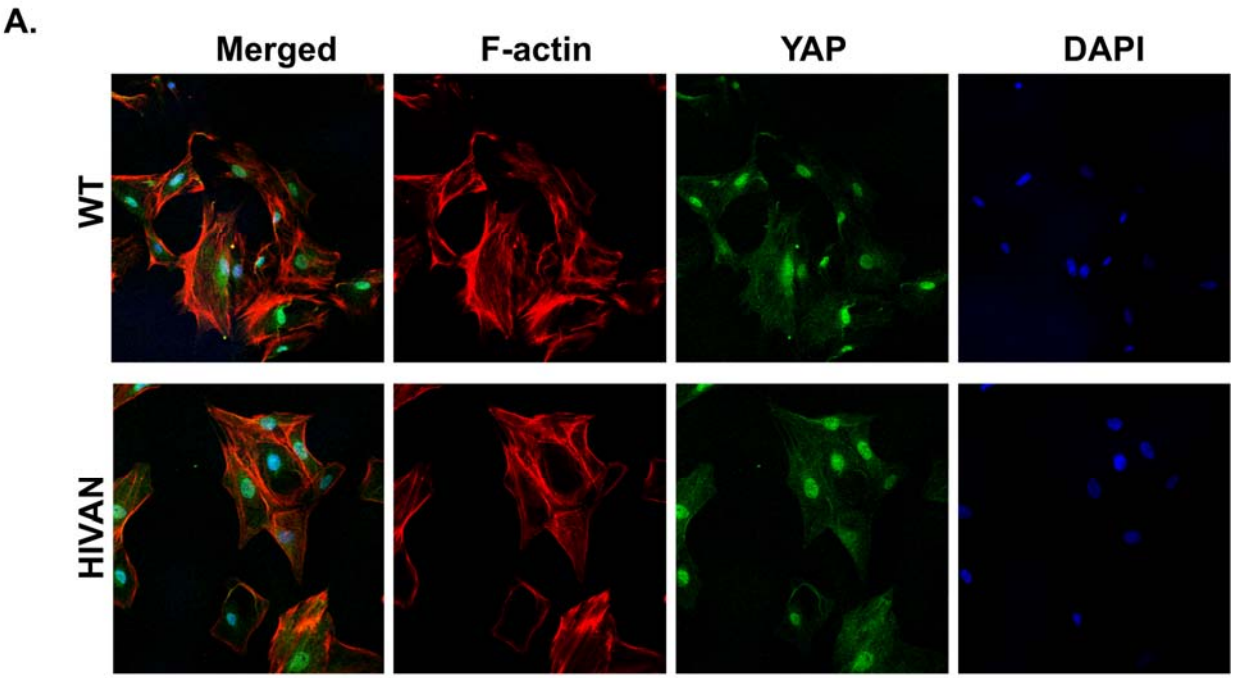

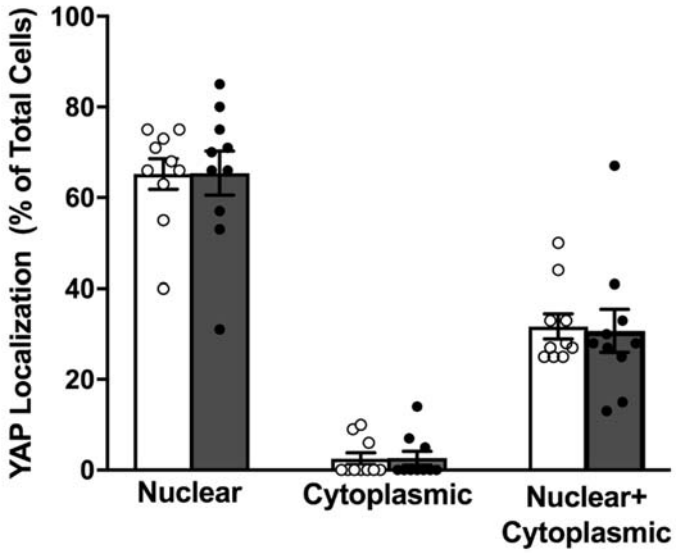

Figure S5. Nuclear versus cytoplasmic localization of YAP in normal and Tg26 mesangial cells. A) Cells were plated on type I collagen-coated glass coverslips and stained for YAP (green), rhodamine-phalloidin (red, F-actin), and DAPI (blue) for nuclei, and imaged using confocal microscopy (40X). B) Bar graph shows quantitation of nuclear, cytoplasmic, and

nuclear+cytoplasmic localization YAP distribution in WT (white bar, mean ± SE) and Tg26 mesangial cells (filled bar, mean ± SE). For each cell type, cells in ten fields were assigned a nuclear, cytoplasmic, or nuclear+cytoplasmic distribution, and percentages determined from N>100 total number of cells.

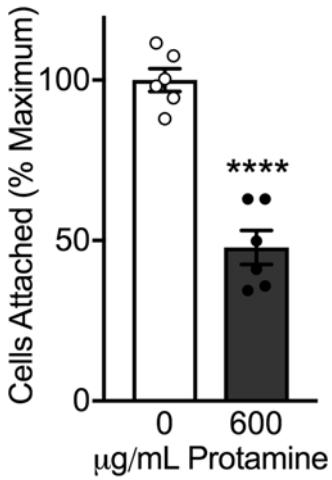

Figure S6. Effects of protamine on podocyte cell adhesion to collagen coated plates. Cell adhesion was quantified using crystal violet staining of attached cells. Bar represents the mean of four experiments with triplicate wells in each experiment. Values are expressed as a percentage of the maximum OD reading for an experiment (highest value for WT), then normalized to average control no protamine values. ****P< 0.0001 versus control by paired t test.

Supplementary Methods

Antibodies and reagents. The following antibodies were used for Western blotting and immunocytochemistry: Phospho-paxillin, paxillin, vinculin 7F9 (company), YAP 63.7 (company), rhodamine-phalloidin (Invitrogen), CD61-APC (clone 2C9.G2, Biolegend), CD51-PE (clone RMV-7, Biolegend), CD29-PB (clone HMB1-1, Biolegend), CD49a-BV711 (clone HA 31/8, BD Biosciences), CD49c-PE (BD Biosciences), CD16-FC block (clone 93, Biolegend), Propidium Iodide (Tonbo Biosciences). Type I rat tail collagen was from Corning (Corning, NY).

Tg26 mouse and protamine models. The transgenic mouse models of HIVAN FVB/N-Tg(HIV)26Aln/PkltJ, (Jackson Laboratory, strain #022354) commonly referred to as "Tg26" is on the FVB/N background and expresses a replication-defective HIV proviral genome (Δ*gag*, *pol*) under the native HIV-1 promoter[1, 2]. Podocyte cell lines derived from normal and Tg26 transgenic mice bred with H-2K^b-tsA58 Immortomice were described previously[3]. The WT podocytes were studied after differentiation (10 – 12 days at 38˚C when their morphology was characteristic of differentiated cells with growth arrest and increased synaptopodin expression[4]. Tg26 cells were studied after 10 - 12 days at 38˚C, but one of their characteristics is failure to differentiate. Primary podocytes were gown out from isolated glomeruli in RPMI 1640 on type I collagen with 10% FCS for 3 – 5 days, the cellular material resuspended and cells isolated by passage through a 33 μm pore sieve to remove glomerular remnants. The cells were assessed for synaptopodin expression and used for studies[5]. Mesangial cells from normal and Tg26 mice were immortalized following isolation from glomeruli using lentiviral expression of a ts SV40 large T antigen (pLenti-SV40-T-tsA58). For the protamine model, isolated glomeruli or normal podocytes were treated with protamine in tissue culture medium (RPMI 1640) at the concentrations indicated for 1 - 2 hrs before studies were performed[6, 7].

Mice were monitored for development of renal disease using urine dipsticks and general examination. At the time of sacrifice, blood and urine were obtained for measurement of BUN and urine protein/creatinine ratio. Tg26 mice do not develop renal disease at predictable times following birth, but sporadically. In order to have groups of mice that are comparable in disease stage, they were characterized based on several observable criteria. Characteristics of progressive disease were defined by mouse physical appearance, gross pathology of dissected kidneys, and level of proteinuria by dipstick. Mice with minimal proteinuria (1+ on dipstick), normal appearance and activity, along with grossly normal appearing kidneys at the time of sacrifice were classified as Stage I, mice with a higher level of proteinuria (2+ on dipstick), normal activity, but granular-appearing kidneys (indicative of tubular cysts) at the time of sacrifice were classified as Stage II, and mice that exhibited clinical signs of renal failure including reduced activity and peripheral edema, with pale, blistered, enlarged kidneys at the time of sacrifice were classified as Stage III.

Isolation of glomeruli. Glomeruli were prepared using a standard differential sieving technique[8, 9]. Glomeruli from the normal and Tg26 mice were prepared using a modification of the method of Takemoto[9, 10]. Glomeruli were maintained in DMEM with 10% fetal bovine serum at room temperature. All procedures were in compliance with NIH guidelines for the use and care of laboratory animals.

Cell culture. Conditionally immortalized normal mouse podocytes (WT) and conditionally immortalized Tg26 podocytes ("HIVAN" podocytes) were propagated in RPMI 1640 medium with 10% FBS and 10 units/ml recombinant mouse γIFN (Cell Sciences, Newburyport, MA) at 33˚C.

Conditionally immortalized normal and Tg26 mesangial cells were propagated in DMEM/F12 with 20% FBS with 1X Insulin-Transferrin-Selenium (Gibco, Life Technologies) and 10 units/ml γIFN at 33˚C. The cells were induced to differentiate by removing the γIFN, plating them on type I collagen-coated plastic dishes, raising the temperature to 37˚C and growing them for 10 – 14 days. Differentiation of podocytes was assessed by measuring expression of synaptopodin[11]. Differentiated podocytes were the suspended and plated on collagen-coated coverslips, gels, or multi-well plates as needed for individual experiments. Primary podocytes from WT and Tg26 mice were prepared from isolated glomeruli[5, 12]. Glomeruli were prepared by sieving cultured for 5 days in RPMI 1640 and 10% FCS. The cells growing our form glomeruli were epithelial cells and were trypsinized and passed through sieves with a 25-sm pore size to remove the remaining glomerular cores. The cells were re-plated on type I collagen and cultured in RPMI 1640 with 10% FCS.

Histology. Formalin-fixed, paraffin-embedded kidney tissue was sectioned at 3 μm, and sections were stained with Masson's trichrome and Periodic acid-Schiff (PAS) stains. Stained tissue sections were examined and digital images collected under brightfield microscopy with an Olympus BX-60 microscope equipped with Q-imaging Retiga 2000R imaging system.

Microindentation. For measurement of the elastic modulus of a glomerulus, an isolated glomerulus is placed on a glass slide and localized under the probe of a microtensiometer (Kibron Inc, Helsinki, Finland). The probe is lowered onto the glomerulus at a rate of 320 nm/second using an Eppendorf micromanipulator (Eppendorf, Germany). At intervals of 2 μm, voltage is recorded from the read-out of the microtensiometer. Force is calculated from the voltage, and used to calculate an elastic modulus for the glomerulus. The mathematical model for this geometry of a flat probe indenting a spherical sample is discussed in[13, 14]. In the formula,

$$E_{Mod} = \frac{F(1 - \nu^2)}{(4/3\sqrt{r})\sigma^{3/2}}$$

F (force) is calculated from voltage in μN, ν is the Poisson ratio (assumed to be 0.5), r is the radius of a glomerulus (40 μm), σ = ΔZ-F/K where z = displacement (μm, measured by the micromanipulator), and K is the spring constant for the probe (1.2 μN/μm). Curves were calculated from the first 10 – 20 μm following contact of the probe with the glomerulus. From eight to 15 glomeruli were measured for a data point. Curves were generated and analyzed using GraphPad Prism 6 software[13, 14].

The probe is flat, 500 μm in diameter, and deforms the surface of a glomerulus which is composed of capillaries rather than a small region of a cell on the surface of a capillary like AFM. The compression is 15 μm, less than the diameter of two capillaries, so micro-indentation measurements reflect the state of the capillary wall which is primarily determined by the behavior and state of podocytes, and should not be affected by mesangial cells because the compression would not encroach on mesangial cells[13, 14].

qRT-PCR. Differentiated podocyte and mesangial cell lines were cultured on acrylamide gels of variable stiffness for 24 hours. Cells were harvested and RNA was extracted with a Qiagen RNEasy extraction kit. cDNA was generated using an ABI First Strand synthesis kit (Invitrogen) and qRT-PCR was performed using SYBR Green master mix (Thermofisher) with theStepOne Real Time PCR System (Applied Biosystems) per manufacturer's instructions. Gene expression was measured with the following oligos:
Filamin- fwd: GATGCACCGTGGAAGAAAAT, rev: GTGGGTCTTTGGTTGTGCTT

Myh9- fwd: GAGCGATACTACTCAGGGCTT, rev: TCTTGCTCTTGTGTGAGGAGG
WT-1- fwd: TGAAAAGCCCTTCAGCTGTC, rev: GGAGTTTGGTCATGTTTCTCT
Podocin- fwd: TGAGGATGGCGGCTGAGAT; rev: GGTTTGGAGGAACTTGGGT1
mCOL1A1- fwd: CCCCGGCCCCATTGGTAACG; rev: AGGGACCAGGGGGACCGAC
mCOL1A2- fwd: ACGCGGACTCTGTTGCTGCT; rev: GCGGGACCCCTTTGTCCACG
COL4a1- fwd: CAAGGTTCACCAGGGCTTAT; rev: ACCTGGGTCTCCTTTGTCAC
COL4a2-fwd: GTCAAGGGAGACATCGGAGT; rev: CTCCTGGAGTACCCTTCTCG
Lox- fwd: CATGGTGGGCGACGACCCCT; rev: GGTCCGGGAGACCGTACTGGA
LOXL1- fwd:CAGCGTGGGTAGTGTGTACC; rev: TACAGATGGGCTCTCTGCAC
LOXL2- fwd:GGAAAGCCTACAAGCCAGAG; rev: GCAGATACCAGGTCCCACTT
LOXL3- fwd:TCACAGCTGAGGACTGTTCC; rev:ATCCCTATTTGCACCTCGAC
LOXL4- fwd:GCTCTGCTCACACACCAGAT; rev: CTTCTTGGTGCTCCTTGTCA
GAPDH fwd: CTCATGACCACAGTCCATGC; rev: CACATTGGGGGTAGGAACAC

Measurement of cell adhesion. Integrin-dependent and integrin-independent adhesion was measured by plating equal numbers of cells ($2x10^4$ cells/well) in collagen- (10 μg/ml) or poly-lysine-coated (10 μg/ml) 96 well plates in triplicate. After 30 min, the plates were washed, fixed in formalin for 10 min, and the cells stained with 0.01% crystal violet for 30 min. The stain was solubilized with methanol-acetic acid, and the plates read in a microplate reader (absorbance at 590 nm)[15].

Paxillin phosphorylation. For the phospho-paxillin assays, differentiated HIVAN or WT podocytes were serum-deprived, suspended and plated on 35 mm dishes coated with type 1 collagen (10 μg/ml) for periods of 15, 30, 45, 60, 120, and 180 minutes. The cells were extracted in HME buffer, the extracts normalized for protein, and phospho-paxillin measured as the ratio of phospho-paxillin to total paxillin at each time point.

Immunofluorescence confocal microscopy. The cells were plated on collagen-coated coverslips for the periods of time shown, washed with PBS, fixed with 4% paraformaldehyde, permeabilized in 0.2% Triton-x-100 and stained with an anti-vinculin or anti-paxillin antibody as indicated, and Texas Red-labeled phalloidin. The secondary antibody was green Alexa Fluor 488 goat-anti-rabbit IgG. Cells were then visualized using a Zeiss fluorescence microscope (Model LSM-5 Pascal) and imaged by AxioVision Viewer 3.0.

Fabrication and Measurements on variable stiffness gels. Variable stiffness polyacrylamide gels were prepared as previously described[16]. Gels were cast to specific elasticities by varying the concentration of Bis-acrylamide added. Gels were coated with 50mM sulfosuccinimidyl 6 (4'-azido-2'-nitrophenyl-amino) hexanoate (Sulfo-SANPAH, Pierce) in HEPES, pH 8.5 buffer and exposed to UV light for 10 min to photoactivate the crosslinker. Sulfo-SANPAH was removed, washed with HEPES buffer, and incubated with 0.2mg/mL type I collagen (Sigma) solution overnight at 4°C. Prior to use, gels were washed with PBS.

Flow Cytometry and measurement of integrin cell surface expression.
Wild-type and HIVAN podocytes cultured on Collagen Type I were differentiated 7 days and harvested in suspension. Cells (up to $1x10^6$ events) were stained with antibodies against Itgα1, Itgα3, Itgαv, Itgβ1, Itgβ3 and fixed in 1% paraformaldehyde (PFA) (Electron Microscopy Sciences, Hatfield, PA). Cells were collected on a BD Fortessaand. Data were analyzed with Flowjo Software (Treestar, Ashland, OR, USA)[17].

Atomic force microscopy (AFM). AFM was done with a DAFM-2X Bioscope (Veeco, Woodbury, NY) mounted on an Axiovert 100 microscope (Zeiss, Thornwood, NY) using silicon nitride cantilevers (196 mm long, 23 mm wide, 0.6 mm thick) with a bead tip (1 mm diameter) for indentation. The spring constant of the cantilever, calibrated by resonance measurements, was typically 0.06 N/m (Novascan, Ames, IA)[16]. A grid with 300 mm divisions was placed lengthwise beneath the gel, and ~3–4 cell/gel stiffness measurements are made within each division. Correlation between cell and gel stiffness was determined by indenting the cells at three distinct points and the gel at three points proximal to the attached cell. To quantify stiffness (elastic modulus), the first 500 nm of tip deflection was fit with the Hertz model for a sphere:

$$f_{bead} = k * d_{cantilever} = \frac{4}{3}\frac{E}{1-\nu^2}\sqrt{R}\delta^{\frac{3}{2}}$$

where f_{bead} is the force on the bead, k is the spring constant of the cantilever, $d_{cantilever}$ is the deflection of the cantilever measured by the AFM, E is the Young's modulus, v is the Poisson ratio, R is the radius of the bead, and δ is the vertical indentation of the material. δ is determined by subtracting $d_{cantilever}$ from the distance traveled by the cantilever during the indentation process. Previous studies have shown that this simple approximation, although not exact for our conditions, is correct within a small fraction (<15%) of values determined by conventional rheometry of identical gels[16]. Phase contrast images of cells, including those measured by AFM, were analyzed using Image J to determine adherent area.

Three-dimensional collagen matrix contraction assay. Methods for preparing cell-containing collagen matrices have been described previously[18]. Briefly, collagen matrices ($2x10^5$ cells/200μL gel) were polymerized for 1 hour at 37°C. The gels were released from their substrates to float in RPMI 1640 medium with or without 20% FBS for four hours and then fixed with 3.7% paraformaldehyde/PBS. Images of collagen matrices were obtained with an Epson photo scanner. Gel area was analyzed using ImageJ, and reduction I area was calculated as: original area (12 mm diameter circle) – area after treatment. Relative gel area reduction was normalized to the WT control condition. Statistical analyses were performed using GraphPad Prism software.

Immunofluorescence and Confocal Microscopy Analysis. Cells were seeded onto collagen-coated glass coverslips overnight, fixed with paraformaldehyde/PBS, blocked with 3% BSA/PBS, and permeabilized with 0.5% Triton X-100/PBS for 5 minutes. Cells on coverslips were stained using standard procedures, mounted onto glass slides with Fluoromount-G with DAPI, and microscopic images were collected with a confocal microscope (LSM880, ZESS). Acquired images were processed with LSM Image Browser software (ZEN 2012). For cell staining in 3D matrix, the same procedures were followed, but after fixation of floating gels, permeability was increased with 0.5% Triton X-100/PBS for 20 minutes.

Statistical Methods. Analyses of statistical significance were performed with GraphPad Prism 6.0. For comparisons of two groups, t-test was used to determine significance. For comparisons of average values of greater than two groups, significance was determined by 1-way ANOVA, with Dunnett's posthoc test for comparison to control WT group, Tukey's multiple comparisons test for comparisons between all groups. For comparisons of groups of data, significance was determined by 2-way ANOVA with Sidak's multiple comparisons test.

References.

1. Kopp, JB, Klotman, ME, Adler, SH, Bruggeman, LA, Dickie, P, Marinos, NJ, Eckhaus, M, Bryant, JL, Notkins, AL, Klotman, PE: Progressive glomerulsclerosis and enhanced renal accumulation of basement membrane components in mice transgenic for human immunodeficiency virus type 1 genes. *Proceedings of the National Academy of Science,* 89**:** 1577-1581, 1992.
2. Bruggeman, LA, Dikman, S, Meng, C, Quaggin, SE, Coffman, TM, Klotman, PE: Nephropathy in human immunodeficiency virus-1 transgenic mice is due to renal transgene expression. *JClinInvest,* 100**:** 84-92, 1997.
3. Schwartz, EJ, Cara, A, Snoeck, H, Ross, MD, Sunamoto, M, Reiser, J, Mundel, P, Klotman, PE: Human immunodeficiency virus-1 induces loss of contact inhibition in podocytes. *JASN,* 12**:** 1677-1684, 2001.
4. Tandon, R, Levental, I, Huang, C, Byfield, FJ, Ziembicki, J, Schelling, JR, Bruggeman, LA, Sedor, JR, Janmey, PA, Miller, RT: HIV infection changes glomerular podocyte cytoskeletal composition and results in distinct cellular mechanical properties. *Am J Physiol Renal Physiol,* 292**:** F701-710, 2007.
5. Mundel, P, Reiser, J, Zuniga, A, Borja, M, Pavenstadt, H, Davidson, GR, Kriz, W, Zeller, R: Rearrangements of the cytoskeleton and cell contacts induce process formation during differentiation of conditionally immortalized mouse podocyte lines. *Experimental cell research,* 236**:** 248-258, 1997.
6. Vassiliadis, J, Bracken, C, Matthews, D, O'Brien, S, Schiavi, S, Wawersik, S: Calcium mediates glomerular filtration through calcineurin and mTORC2/Akt signaling. *JASN,* 22**:** 1453-1461, 2011.
7. Buvall, L, Wallentin, H, Sieber, J, Andreeva, S, Choi, HY, Mundel, P, Greka, A: Synaptopodin Is a Coincidence Detector of Tyrosine versus Serine/Threonine Phosphorylation for the Modulation of Rho Protein Crosstalk in Podocytes. *Journal of the American Society of Nephrology : JASN,* 28**:** 837-851, 2017.
8. Schlondorff, D: Preparation and study of isolated glomeruli. *Methods in Enzymology,* 191**:** 130-140, 1987.
9. Takemoto, M, Asker, N, Gerhart, G, Lundkvist, A, Johansson, BR, Saito, Y, Betsholz, C: A new method for large scale isolation of kidney glomeruli from mice. *AmJPath,* 161**:** 799-805, 2002.
10. Takemoto, M, He, L, Norlin, J, Patrakka, J, Xiao, Z, Petrova, T, Bondjers, C, Asp, J, Wallgard, C, Sun, Y, Samuelsson, T, Mostad, P, Lundin, S, Miura, N, Sado, Y, Alitalo, K, Quaggin, SE, Tryggvason, K, Betsholtz, C: Large-scale identification of genes implicated in kidney glomerulus development and function. *EMBO,* 25**:** 1160-1174, 2006.
11. Shankland, SJ, Pippin, JW, Reiser, J, Mundel, P: Podocytes in culture: past, present, and future. *Kidney international,* 72**:** 26-36, 2007.
12. Mundel, P, Reiser, J, Kriz, W: Induction of differentiation in cultured rat and human podocytes. *Journal of the American Society of Nephrology : JASN,* 8**:** 697-705, 1997.
13. Levental, I, Levental, KR, Klein, EA, Assoian, R, Miller, RT, Wells, RG, Janmey, PA: A simple indentation device for measuring micrometer-scale tissue stiffness. *Journal of Physics: Condensed Matter,* 22**:** 191420, 2010.
14. Embry, AE, Mohammadi, H, Niu, X, Liu, L, Moe, B, Miller-Little, WA, Lu, CY, Bruggeman, LA, McCulloch, CA, Janmey, PA, Miller, RT: Biochemical and

Cellular Determinants of Renal Glomerular Elasticity. *PloS one,* 11**:** e0167924, 2016.
15. Miao, H, Strebhardt, K, Pasquale, EB, Shen, TL, Guan, JL, Wang, B: Inhibition of integrin-mediated cell adhesion but not directional cell migration requires catalytic activity of EphB3 receptor tyrosine kinase. *Journal of Biological Chemistry,* 280**:** 923-932, 2005.
16. Byfield, FJ, Wen, Q, Levental, I, Nordstrom, K, Durian, DJ, Arratia, PE, Miller, RT, Janmey, PA: Absence of filamin A prevents cells from responding to substrate stiffness on gels coated with collagen but not fibronectin. *BiophysJ,* 96**:** 5095-5102, 2009.
17. Cravens, PD, Hussain, RZ, Miller-Little, WA, Ben, LH, Segal, BM, Herndon, E, Stuve, O: IL-12/IL23-p40 is highly expressed in secondary lymphoid organs and the CNS during all stages of EAE, but its deletion does not affect disease perpetuation. *PloS one,* 11**:** e0165248, 2016.
18. Liu, ZN, Ho, CH, Grinnell, F: The different roles of myosin IIA and myosin IIB in contraction of 3D collagen matrices by human fibroblasts. *Experimental Cell Research,* 326**:** 295-306, 2014.